*Kuwait J. Sci. Eng.* **30**(2) pp. 95-108, 2003

# Shape and depth solutions form third moving average residual gravity anomalies using the window curves method

EL-SAYED M. ABDELRAHMAN,
TAREK M. EL-ARABY AND KHALID S. ESSA

*Geophysics Department, Faculty of Science, Cairo University, Giza, Egypt.*

## ABSTRACT

In this paper, we have used the window curves method to simultaneously determine the shape factor and the depth of a buried structure from third moving average residual gravity anomalies. The method involves using a relationship between the shape factor and the depth to the source, and a combination of windowed observations. This method can be applied not only to "true residuals" but also to the Bouguer gravity data consisting of the combined effect of a residual component due to a purely local structure and a regional component represented by a deep-seated structure. The method is applied to theoretical data with and without random errors and tested on a known field example from the U.S.A. In all cases, the shape and depth solutions obtained are in good agreement with the actual ones.

**Keywords:** gravity interpretation; third moving average method; window curves.

## INTRODUCTION

The main purpose of gravity surveys is to map rocks possessing lateral density variations within the Earth's crust and/or the upper mantle which cause anomalies in the intensity of the Earth's gravity field. Profiles of gravity anomalies are usually used qualitatively to help in regional geologic interpretation. Often the existence of interfering sources is a problem in the use of quantitative methods of evaluation (Abdelrahman *et al.* 2001a). It is under these circumstances that the interpretation of gravity data must involve removal of unwanted field components to isolate the desired anomaly which is known as regional-residual separation. This operation includes graphical methods (Nettleton, 1976), least-squares techniques (Abdelrahman *et al.* 1985), and radial weight methods (Griffin 1949). The derived residual and regional gravity anomalies are then geologically interpreted to estimate the shape and depth of the buried structure, often without accounting for the uncertainities introduced by the separation process. When the above techniques are applied to observed data, they may distort the shape of the gravity anomalies. Thus residual and

regional gravity anomalies generally yield unreliable geological interpretation (Hammer 1977).

To overcome the above difficulties, several methods have been developed to estimate the shape and depth of the buried structure from gravity data. Abdelrahman and El-Araby (1993) show that correlation factors between successive least-squares residual gravity anomalies can be used to estimate the depth and shape of the buried structure. Abdelrahman and El-Araby (1996) and Abdelrahman *et al.* (2001b) indicate that the window curves method can be used to simultaneously determine the shape and the depth of the buried structure from first and second moving average residuals obtained from gravity data using successive window lengths. The accuracy of the result obtained by the methods of Abdelrahman and El-Araby (1996) and Abdelrahman *et al.* (2001b) depends on the degree of complexity of the regional gravity field present in the data. However, effective quantitative procedures using also the window curves method from the third moving residual gravity anomalies are yet to be developed. The advantage of using the third moving average method over the first and the second ones is that it can adequately remove the gravity effect of the deep-seated structure and determine the correct parameters of the shallow structure.

The aim of the present study is to develop a simple method for analysis of gravity data due to the discrete sources. The analysis stems from third moving average residual calculations that can be used to determine the shape and depth of the causative bodies using the window curves method. The validity of the method is tested on theoretical examples and a field example from Texas, U. S. A.

## FORMULATION OF THE PROBLEM

The general gravity anomaly expression produced by a semi-infinite vertical cylinder, a horizontal cylinder, and a sphere is given by Abdelrahman and El-Araby (1993) as

$$g(x_i, z, q) = \frac{A}{(x_i^2 + z^2)^q}, \tag{1}$$

where $q$ is the shape (shape factor ), $z$ is the depth, $x$ is the position coordinate, and $A$ is an amplitude coefficient related to the radius and density contrast of the buried structure. Examples of the shape factor for the semi-infinite vertical cylinder, horizontal cylinder, and sphere are 0.5, 1.0, and 1.5, respectively.

The moving average (grid) method is an important yet simple technique for the separation of gravity anomalies into residual and regional components. The basic theory of the moving average methods is described by Griffin (1949), Agocs (1951),

Abdelrahman and El-Araby (1996), and Abdelrahman *et al*. (2001b).

Let us consider seven observation points $(x_i - 3s,\ x_i - 2s,\ x_i - s,\ x_i,\ x_i + s,\ x_i + 2s,$ and $xi + 3s)$ along the anomaly profile where $s = 1, 2, ..., M$ spacing units and is called the window length. The first moving average regional gravity field $Z(x_i, z, q, s)$ is defined as the average of $g(x_i - s, z, q)$ and $g(x_i + s, z, q)$, which for the simple shapes mentioned above can be written as

$$Z(x_i, z, s) = \frac{A}{2}\left\{((x_i - s)^2 + z^2)^{-q} + ((x_i + s)^2 + z^2)^{-q}\right\}. \tag{2}$$

The first moving average residual gravity anomaly $R_1(x_i, z, q, s)$ at the point $x_i$ is defined as (Abdelrahman & El-Araby 1993).

$$R_1(x_i, z, q, s) = \frac{A}{2}\left[2(x_i^2 + z^2)^{-q} - \left(((x_i - s)^2 + z^2)^{-q} + ((x_i + s)^2 + z^2)^{-q}\right)\right]. \tag{3}$$

The second moving average residual gravity anomaly $R_2(x_i, z, q, s)$ at the point $x_i$ is (Abdelrahman *et al*. 2001b)

$$R_2(x_i, z, q, s) = \frac{A}{2}\Big[6(x_i^2 + z^2)^{-q} - 4((x_i - s)^2 + z^2)^{-q} - 4((x_i + s)^2 + z^2)^{-q} + ((x_i - 2s)^2 + z^2)^{-q} + ((x_i + 2s)^2 + z^2)^{-q}\Big]. \tag{4}$$

The third moving average residual gravity anomaly $R_3(x_i, z, q, s)$ at any point $x_i$ is

$$R_3(x_i, z, q, s) = \frac{A}{8}\Big[20(x_i^2 + z^2)^{-q} - 15((x_i + s)^2 + z^2)^{-q} - 15((x_i - s)^2 + z^2)^{-q} + 6((x_i + 2s)^2 + z^2)^{-q} + 6((x_i - 2s)^2 + z^2)^{-q} - ((x_i + 3s)^2 + z^2)^{-q} - ((x_i - 3s)^2 + z^2)^{-q}\Big]. \tag{5}$$

For all shape factors $(q)$, (5) gives the following value at $x_i = 0$

$$A = \frac{4R_3(0)}{[10z^{-2q} - 15(s^2 + z^2)^{-q} + 6(4s^2 + z^2)^{-q} - (9s^2 + z^2)^{-q}]}. \tag{6}$$

Using (5) and (6), we obtain the following normalized equation at $x_i = s$

$$\frac{R_3(s)}{R_3(0)} = \frac{[26(s^2 + z^2)^{-q} - 16(4s^2 + z^2)^{-q} + 6(9s^2 + z^2)^{-q} - 15z^{-2q} - (16s^2 + z^2)^{-q}]}{[20z^{-2q} - 30(s^2 + z^2)^{-q} + 12(4s^2 + z^2)^{-q} - 2(9s^2 + z^2)^{-q}]}. \tag{7}$$

Equation (7) is independent of the amplitude coefficient (A). Let $F = R_3(s)/R_3(0)$. Then from (7) we obtain

$$z = \left[\frac{-15}{F * P(s,z,q) + W(s,z,q)}\right]^{1/2q}, \tag{8}$$

where

$$P(s,z,q) = \left[20z^{-2q} - 30(s^2+z^2)^{-q} + 12(4s^2+z^2)^{-q} - 2(9s^2+z^2)^{-q}\right],$$

and

$$W(s,z,q) = \left[16(4s^2+z^2)^{-q} - 6(9s^2+z^2)^{-q} + (16s^2+z^2)^{-q} - 26(s^2+z^2)^{-q}\right].$$

Equation (8) can be used not only to determine the depth but also to simultaneously estimate the shape of the buried structure, as will be illustrated by theoretical and field examples.

## THEORETICAL EXAMPLES

### Noise free data

The composite gravity anomaly in mGals of Figure 1 consisting of the combined effect of a shallow structure (horizontal cylinder with 3 km depth) and a deep-seated structure (dipping fault with depth to upper faulted slab = 15 km, depth to lower faulted slab = 20 km, and dip angle of fault plane = 50 degrees) was computed by the following expression

$$\Delta g_1(x_i) = \frac{200}{(x_i^2+3^2)} + 100\left(\tan^{-1}\left(\frac{x_i-5}{15} + \cot(50^\circ)\right) - \tan^{-1}\left(\frac{x_i-5}{20} + \cot(50^\circ)\right)\right)$$

(horizontal cylinder + dipping fault) (9)

The composite gravity field ($\Delta g$) was subjected to our third moving average technique. The third moving average residual value at point $x_i$ is computed from the input gravity data $g(x_i)$ using the following

$$R_3(x_i) = \frac{20g(x_i) - 15g(x_i+s) - 15g(x_i-s) + 6g(x_i-2s) + 6g(x_i+2s) - g(x_i+3s) - g(x_i-3s)}{8}. \tag{10}$$

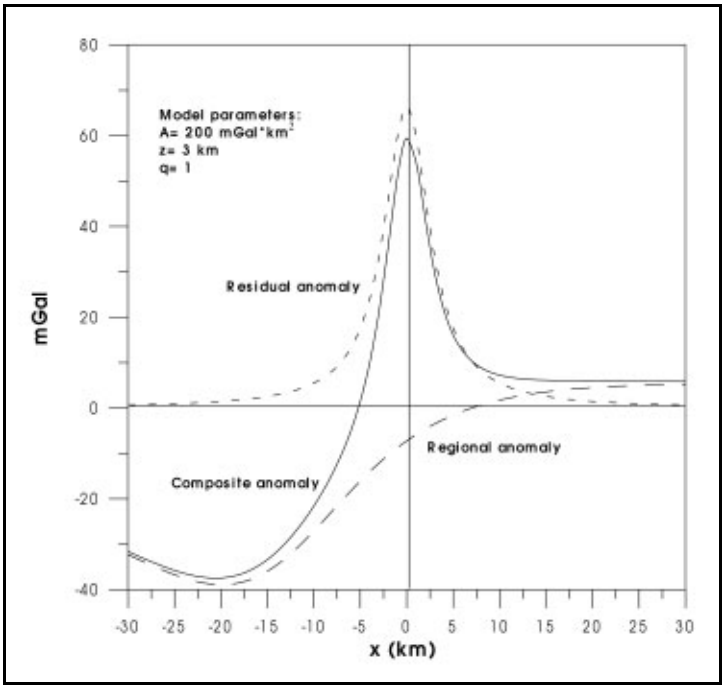


**Fig.1.** Composite gravity anomaly ($\Delta g_1$) of a buried horizontal cylinder and a dipping fault as obtained from (8).

Five successive third moving average windows ($s=$ 2, 3, 4, 5, and 6 km) were applied to input data. Each of the resulting moving average profiles was analyzed by (8). For each window length, a depth value was determined iteratively for all shape values, and a window curve was plotted, illustrating the relation between the depth and shape. We also applied the first moving average method (Abdelrahman & El-Araby 1993) and the second moving average method (Abdelrahman *et al*. 2001b) to the same input data generated from (9). The results in the case of using first, second, and third moving average techniques are shown in Figures 2, 3, and 4, respectively.

In the case of using the first moving average technique, the window curves intersect at a narrow region where $0.55 > q > 0.05$ and $2.5 \text{ km} > z > 1.8$ km (Figure 2). The central point of this region occurs at the location $q=$ 0.26 and $z=$ 2.1 km. On the other hand, in the case of using the second moving average technique, the curves intersect each other nearly at a point where $q=$ 0.75 and $z=$ 2.7 km (Figure 3). Finally, in the case of using the third moving average method (present method), the curves intersect each other at the correct locations $q=$ 1.03 and $z=$ 3.05 km (Figure 4). From these results (Figures 2-4), it is evident that the first and the second moving average methods give erroneous results for the shape and depth solutions, whereas the model parameters obtained from the third moving average method are in excellent agreement with the parameters of the shallow structure given in model (9). The conclusion is inescapable that the third moving average technique gives the best result.

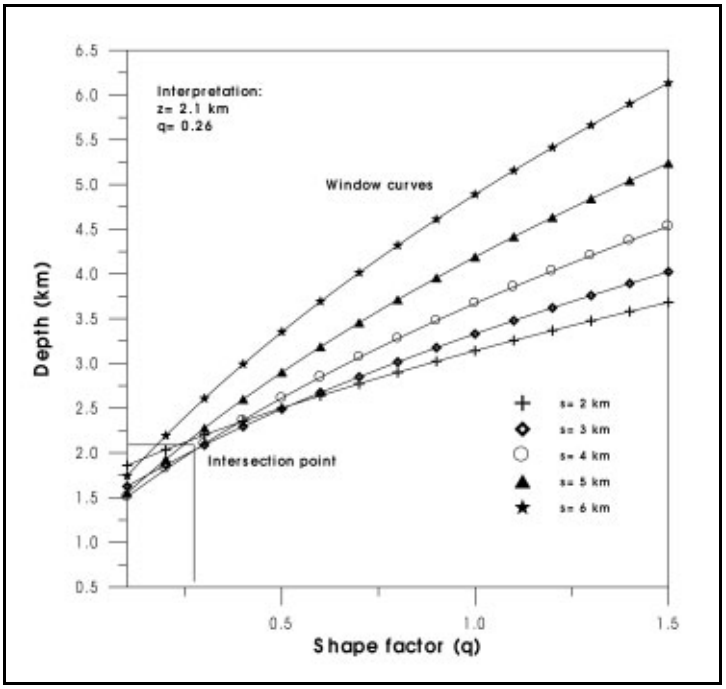


**Fig.2.** Family of window curves of $z$ as $a$ function of $q$ for $s = 2, 3, 4, 5$, and 6 km as obtained from gravity anomaly ($\Delta g_1$) using the first moving average method. Estimates of $q$ and $z$ are, respectively, 0.26, and 2.1 km.

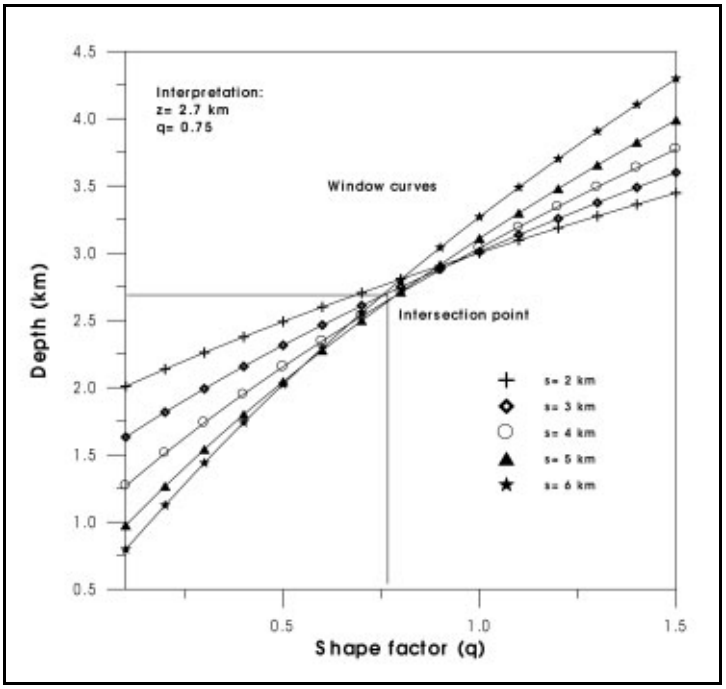


**Fig.3.** Family of window curves of $z$ as $a$ function of $q$ for $s = 2, 3, 4, 5$, and 6 km as obtained from gravity anomaly ($\Delta g_1$) using the second moving average method. Estimates of $q$ and $z$ are, respectively, 0.75, and 2.7 km.

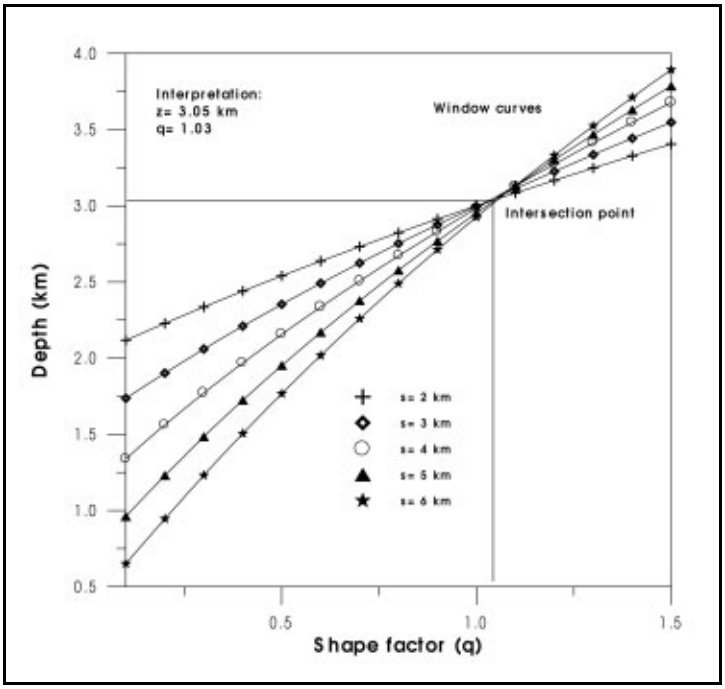


**Fig.4.** Family of window curves of $z$ as $a$ function of $q$ for $s = 2, 3, 4, 5$, and 6 km as obtained from gravity anomaly ($\Delta g_1$) using the present third moving average method. Estimates of $q$ and $z$ are, respectively, 1.03, and 3.05 km.

## Effect of random noise

Random errors were added to the composite gravity anomaly $\Delta g_1(x_i)$ to produce noisy anomaly. In this case, we choose a white random noise with amplitude being 5% of the maximum amplitude variation along the entire profile, so that the noise will be equal along the profile. The noisy anomaly is subjected to a separation technique using only the third moving average method. Five successive third moving average windows were applied to the noisy input data. The results of adapting the same interpretation procedure are shown in Figure 5.

Figure 5 shows that the window curves intersect at approximately $q = 1.09$ and $z = 2.98$ km. The results (Figure 5) are generally in very good agreement with the shape factor and depth parameters shown in (9). This indicates that our method will produce reliable shape and depth estimates when applied to noisy gravity data.

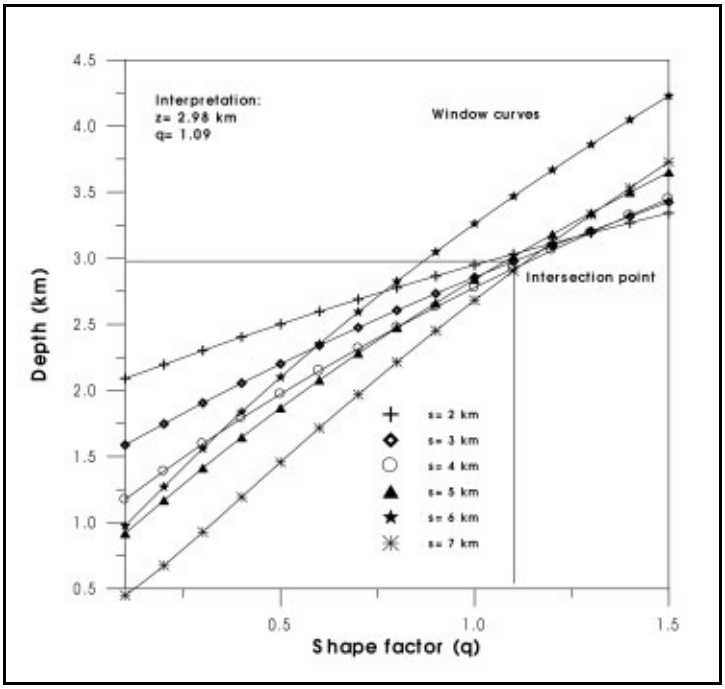


**Fig.5.** Family of window curves of $z$ as $a$ function of $q$ for $s = 2, 3, 4, 5, 6,$ and 7 km as obtained from gravity anomaly ($\Delta g_1$) after adding 5% random errors to the data using the present third moving average method. Estimates of $q$ and $z$ are, respectively, 1.09, and 2.98 km.

## Extension to a more complex shape

Consider, for example, the gravity field

$$\Delta g_2(x_i) = 15(\tan^{-1}(\frac{1+x_i}{5}) - \tan^{-1}(\frac{-1-x_i}{5})) + \frac{15000}{(x_i^2+20^2)^{3/2}}, \qquad (11)$$

2-D prism with rectangular cross-section + sphere

which represents a composite gravity field consisting of the combined effect of a residual component caused by an infinitely long, horizontal, material plane belt which is used to substitute for a 2-D prism (depth to the center = 5 km and width = 2 km) and a regional component due to a sphere having a depth of 20 km (Figure 6). Adopting the same procedure used in the above examples, the results are shown in Figure 7. It is clear from Figure 7 that the window curves intersect each other approximately at a point where $z =$ 5.1 km and $q =$ 0.87. These results suggest that our interpretation method may be extended to infer a distinction in shape between an infinitely long, horizontal, material plane belt, and a horizontal cylinder.

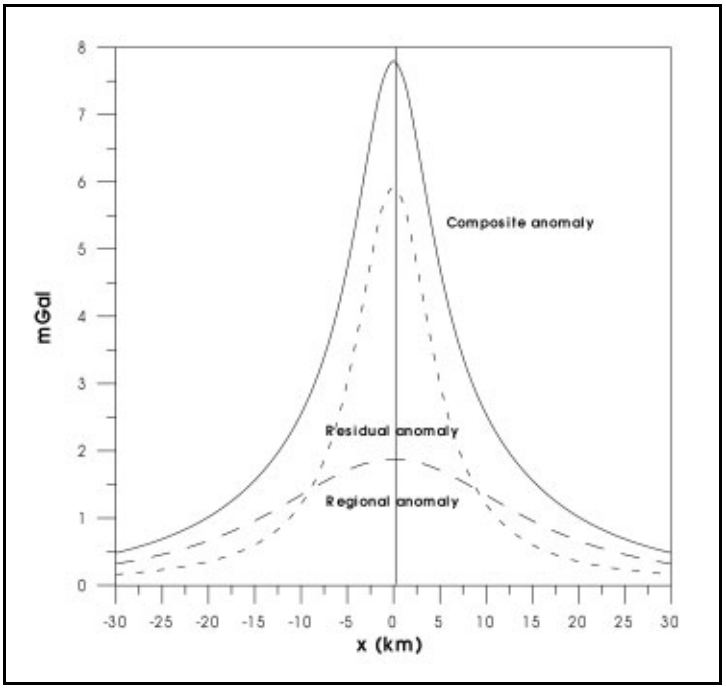


**Fig.6.** Composite gravity anomaly ($\Delta g_2$) of a buried infinitely long, horizontal, material plane belt and a sphere as obtained from (11).

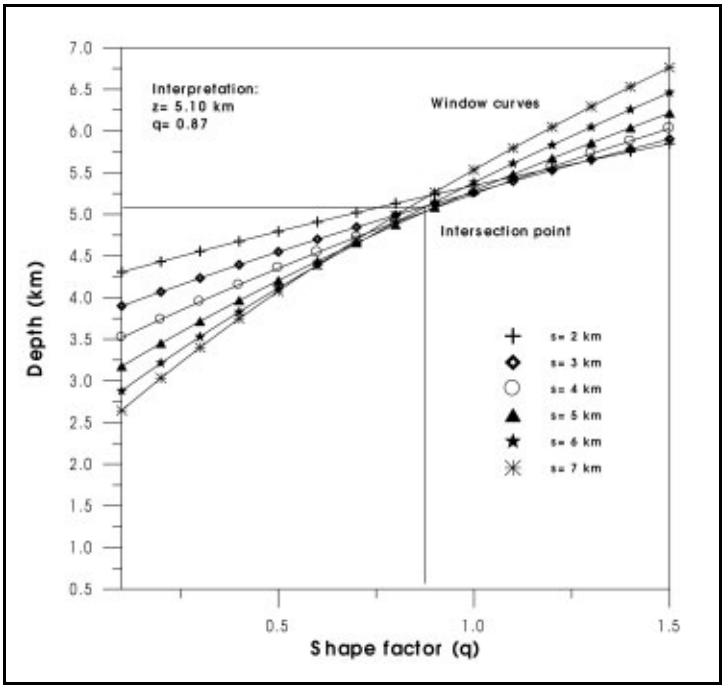


**Fig.7.** Family of window curves of $z$ as $a$ function of $q$ for $s = 2, 3, 4, 5, 6,$ and 7 km as obtained from gravity anomaly ($\Delta g_2$) using the present third moving average method. Estimates of $q$ and $z$ are, respectively, 0.87, and 5.1 km.

## FIELD EXAMPLE

A Bouguer gravity anomaly profile along AÁ of the gravity map of the Humble Salt Dome near Houston (Nettleton, 1962, Fig. 22) is shown in Figure 8. The gravity profile has been digitized at an interval of 0.26 km. The Bouguer gravity anomalies thus obtained have been subjected to a separation technique using the third moving average method. Filters were applied in four successive windows ($s =$ 2.60, 2.86, 3.12, and 3.38 km). In this way, four third moving average residual anomaly profiles were obtained (Figure 9). The same procedure described for the synthetic examples was used to estimate the shape and the depth of the salt dome. The results are plotted in Figure 10. Figure 10 shows that the window curves intersect at a point where the depth is about 4.95 km and at $q = 1.41$. This suggests that the shape of the salt dome resembles a sphere or, more exactly, a three-dimensional source with a hemispherical roof and root. This result is generally in good agreement with the dome form estimated from drilling top and contact (Nettleton, 1976; Figure 8-16).

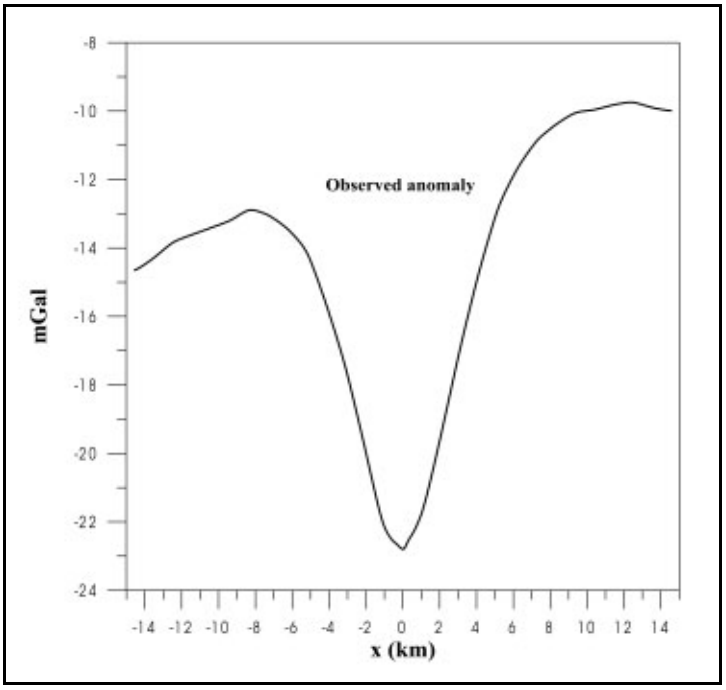


**Fig.8.** Observed gravity profile of the Humble Salt Dome, near Houston, TX, U.S.A. (From Nettleton 1962)

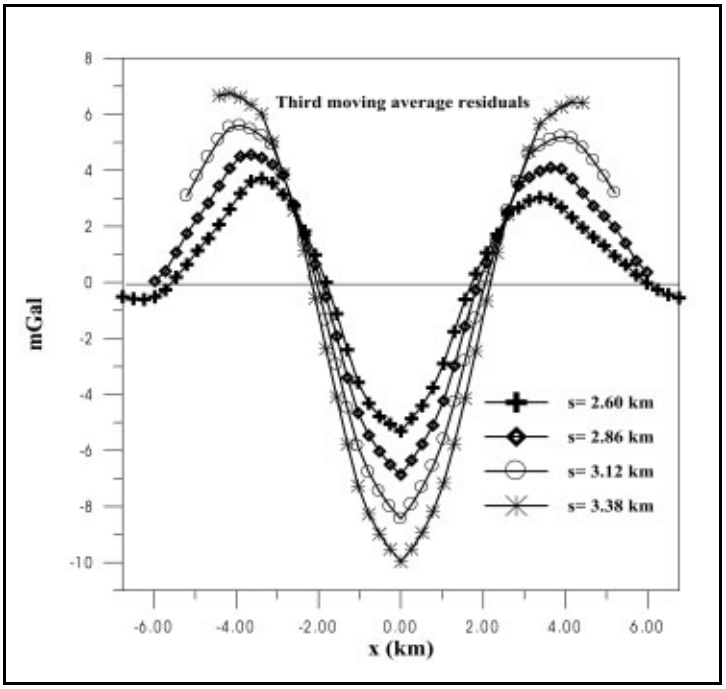


**Fig.9.** Third moving average residual gravity anomalies on line AÁ of the Humble salt dome, for $s$ = 2.60, 2. 86, 3.12, and 3.38 km.

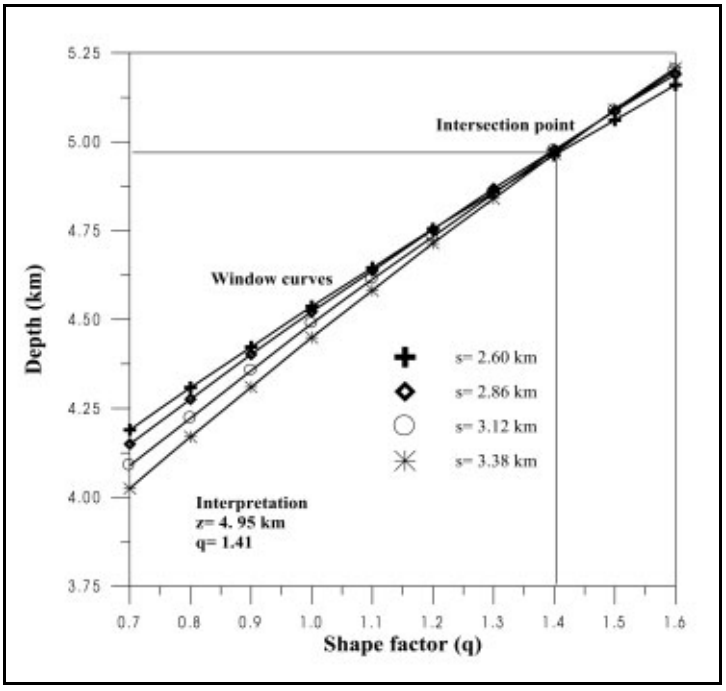


**Fig.10.** Family of window curves of $z$ as $a$ function of $q$ for $s$ = 2.60, 2. 86, 3.12, and 3.38 km as obtained from the Humble gravity anomaly profile using the present approach. Estimates of $q$ and $z$ are, respectively, 1.41 and 4.95 km.

## CONCLUSIONS

The problem of determining the shape and depth from gravity data of long or short profile length can be solved using the present window curves method for simple anomalies. The window curves method is very simple to execute and works well even when the data contains noise. The method involves using simple models convolved with the same third moving average filter as applied to the observed gravity data. As a result, our method can be applied not only to residuals but also to measured gravity data. The advantages of the third moving average method over the first and the second moving average techniques are: (1) the method adequately removes the regional field due to deep-seated structure from gravity data and (2) the method can be applied to large grided data. Theoretical and field examples have illustrated the validity of the method presented.

## ACKNOWLEDGMENTS

The authors thank the editors and two capable reviewers for their excellent suggestions and the thorough review that improved our original manuscript.

## REFERENCES

**Abdelrahman, E. M. & El-Araby, H. M. 1993.** Shape and depth solutions from gravity data using correlation factors between successive least-squares residuals. Geophysics **59**: 1785-1791.

**Abdelrahman, E. M. & El-Araby, T. M. 1996.** Shape and depth solutions from moving average residual gravity anomalies. Journal of Applied Geophysics **36**: 89-95.

**Abdelrahman, E. M., Riad, S., Refai, E. & Amin, Y. 1985.** On the least-squares residual anomaly determination. Geophysics **50**: 473-480.

**Abdelrahman, E. M., El-Araby, H. M., El-Araby, T. M. & Abo-Ezz, E. R. 2001a.** Three least-squares minimization approaches to depth, shape, and amplitude coefficient determination from gravity data. Geophysics **66**: 1105-1109.

**Abdelrahman, E. M., El-Araby, T. M., El-Araby, H. M. & Abo-Ezz, E. R. 2001b**. A new method for shape and depth determinations from gravity data. Geophysics **66**: 1774-1780.

**Agocs, W. B. 1951.** Least-squares residual anomaly determination. Geophysics **16**: 686-696.

**Griffin, W. R. 1949**. Residual gravity in theory and practice. Geophysics **14**: 39-58.

**Hammer, S. 1977**. Graticule spacing versus depth discrimination in gravity interpretation. Geophysics **42**: 60-65.

**Nettleton, L. L. 1962**. Gravity and magnetics for Geologists and Seismologists. APG **46**: 1815-1838.

**Nettleton, L. L. 1976**. Gravity and magnetics in oil prospecting. Mc-Graw Hill Book Co. New York.

***Submitted :*** *15/4/2002*
***Revised :*** *30/3/2003*
***Accepted :*** *2/4/2003*

# تحديد الشكل والعمق من متوسط الحيود التثاقلية المتبقية من الرتبة الثالثة بطريقة النوافذ

**السيد محمد عبدالرحمن و طارق محمد العربي و خالد سيد عيسى**

قسم الجيوفيزياء – كلية العلوم – جامعة القاهرة – الجيزة – مصر

## خلاصة

نستخدم في هذا البحث طريقة منحنيات النوافذ لتحديد الشكل والعمق للأجسام المدفونة تحت الأرض من متوسط الحيود التثاقلية المتبقية من الرتبة الثالثة. وتعتمد الطريقة على إيجاد علاقة بين الشكل والعمق وتشكيل بعض قيم الحيود. ويمكن تطبيق الطريقة ليس فقط على الحيود التثاقلية المتبقية الحقيقية ولكن أيضاً على الحيود التثاقلية الحقلية الناتجة من الأجسام الضحلة والعميقة.

وقد طبقت الطريقة على مجموعات بيانات افتراضية بعضها يحتوي على أخطاء عشوائية وأخرى لا تحتوي على هذه الأخطاء كما تم التأكد من صحة هذه الطريقة بتطبيقها على الحيود التثاقلية لقبة هامبل الواقعة قرب مدينة هيوستن بالولايات المتحدة الأمريكية.